Self-Assembly

International Edition: DOI: 10.1002/anie.201907838
German Edition: DOI: 10.1002/ange.201907838

Discrete π-Stacks from Self-Assembled Perylenediimide Analogues

Feng Su, Guangmei Chen, Peter A. Korevaar, Fangfang Pan, Huijiao Liu, Zongxia Guo, Albertus P. H. J. Schenning, Hui-Jun Zhang, Jianbin Lin,* and Yun-Bao Jiang*

Abstract: *The formation of well-defined finite-sized aggregates represents an attractive goal in supramolecular chemistry. In particular, construction of discrete π-stacked dye assemblies remains a challenge. Reported here is the design and synthesis of a novel type of discrete π-stacked aggregate from two comparable perylenediimide (PDI) dyads (**PEP** and **PBP**). The criss-cross **PEP-PBP** dimers in solution and (**PBP-PEP**)-(**PEP-PBP**) tetramers in the solid state are well elucidated using single-crystal X-ray diffraction, dynamic light scattering, and diffusion-ordered NMR spectroscopy. Extensive π–π stacking between the PDI units of **PEP** and **PBP** as well as repulsive interactions of swallow-tailed alkyl substituents are responsible for the selective formation of discrete dimer and tetramer stacks. Our results reveal a new approach to preparing discrete π stacks that are appealing for making assemblies with well-defined optoelectronic properties.*

A challenging target in supramolecular chemistry is the construction of uniform monodisperse assemblies that exhibit well-defined functional properties.[1] In particular, the controllable assembly of dyes represents a daunting task because π–π interactions, which play a pivotal role in packing and orientation, are bidirectional and lead to the formation of infinite aggregates.[2] However, for in-depth studies on the structure–function relationship of π-conjugated molecular materials, discrete π-stacks with well-defined arrangements are required.[3] By now, when π–π interactions constitute the sole intermolecular force, only a few discrete assemblies of aromatic π systems have been constructed with extra assistance from either coordination cages[4] or through formation of molecular tweezers.[5] Recently, Würthner et al. reported an elegant spacer-encoded self-assembly approach for the formation of well-defined merocyanine dye stacks based on electrostatic dipole–dipole interactions.[6]

In host-guest chemistry, a host and a guest are held together through complementary noncovalent interactions leading to discrete assemblies. To achieve this highly size-complementary assembly, the two components should be chemically distinct. However, in the case of host-guest assemblies, optical transitions and electronic interactions, which are prerequisites for use in optoelectronic devices, are typically absent between these two distinct constituents. Herein, we report that two comparable perylenediimide (PDI) dyads bridged with linkers of different length, exhibiting similar photophysical properties, can uniformly embrace each other through π–π interactions and form stable discrete π-stacks in an analogous formally length complementary manner (Scheme 1 a). This strategy opens the possibility to obtain discrete functional π-aggregates with exact arrangements to provide in-depth insight into the photophysical and optoelectronic properties of π-conjugated materials.

As an important class of organic dyes, PDIs have received great attention for applications in various optoelectronic devices.[7] Recently, we have developed an efficient rhodium-

[*] F. Su, G. Chen, H. Liu, H.-J. Zhang, J. Lin, Y.-B. Jiang
Department of Chemistry, College of Chemistry and Chemical Engineering, Xiamen University
Xiamen 361005 (P. R. China)
E-mail: meghjzhang@xmu.edu.cn
jb.lin@xmu.edu.cn
P. A. Korevaar
Institute for Molecules and Materials, Radboud University
Heyendaalseweg 135, 6525 AJ Nijmegen (The Netherlands)
F. Pan
College of Chemistry, Central China Normal University
Wuhan 430079 (P. R. China)
Z. Guo
College of Chemistry and Molecular Engineering, Qingdao University of Science and Technology, Qingdao 266042 (P. R. China)
A. P. H. J. Schenning
Department of Chemical Engineering and Chemistry, Stimuli-responsive Functional Materials and Devices, Eindhoven University of Technology, Den Dolech 2, 5612 AZ Eindhoven (The Netherlands)
J. Lin, Y.-B. Jiang
MOE Key Laboratory of Spectrochemical Analysis and Instrumentation, Xiamen University, Xiamen 361005 (P. R. China)
Supporting information and the ORCID identification number(s) for the author(s) of this article can be found under: https://doi.org/10.1002/anie.201907838.

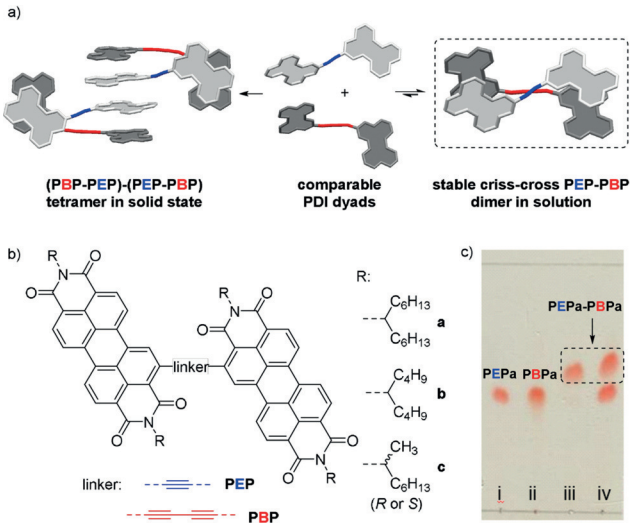

Scheme 1. a) Formation of discrete π-stacks from two comparable PDI dyads that bridged with different length linkers. b) Chemical structures of **PEP** and **PBP**. c) TLC of i) **PEPa**, ii) **PBPa**, iii) **PEPa**/**PBPa** (1:1), iv) **PEPa**/**PBPa** (1:2) (TLC, silica gel; eluent: petroleum ether/ethyl acetate = 5:1).

catalyzed *ortho*-iodination reaction of PDIs. This method can provide key intermediates for the synthesis of various *ortho*-functionalized PDIs without a geometric distortion of the aromatic skeleton.[8] In this article, an *ortho*-ethynylene-bridged PDI dyad (**PEP**) and a slightly longer *ortho*-butadiyne-bridged PDI dyad (**PBP**) were prepared as two π-conjugated molecular look-alikes (Scheme 1b; for details see Scheme S1 in the Supporting Information). Two PDI units are linked to enhance their π–π capabilities.[9] Different swallow-tailed alkyl substituents, including hexylheptyl, butylpentyl, and chiral methylheptyl, at the imide positions are employed to study the solution, solid-state, and helical self-assembly properties. During the synthesis of the PDI dyads, we found that thin layer chromatography (TLC) analysis of a **PEPa** and **PBPa** mixture (1:1 molar ratio) exhibited only one new spot for an assembly, while separation of the assembly and excess of **PBPa** was observed for a 1:2 mixture of **PEPa** and **PBPa** (Scheme 1c). Similar phenomena were also observed for both **PEPb**/**PBPb** and **PEPc**/**PBPc** mixtures. These results suggest that discrete **PEP**-**PBP** complexes with a stoichiometry of 1:1 are formed, and are stable during the TLC separation. We confirmed this 1:1 stoichiometry as well by a Job's plot analysis in methylcyclohexane (MCH; see Figure S1). Furthermore, MALDI TOF mass spectrometry of **PEPa**/**PBPa** (1:1) mainly displayed the peaks belonging to a **PEPa**-**PBPa** aggregate (**1a**) and the free PDI dyads (see Figure S2).

From a chlorobenzene/methanol solution of 1:1 mixture of **PEPb** and **PBPb** with short butylpentyl chains, single crystals suitable for X-ray diffraction analysis were obtained. The crystal structure (space group $P2_1/n$) reveals the formation of a tetramer complex (**PBPb**-**PEPb**)-(**PEPb**-**PBPb**) (**2b**; Figure 1a,b). In this complex, twisting between two PDI units in the PDI dyads takes place (Figure 1c). The dihedral angles between the two PDI units are 80° and 88° for **PEPb** and **PBPb**, respectively. Considering the steric hindrance of bulky swallow-tailed imide substituents, the nearly orthogonal geometries of **PEPb** and **PBPb** along with different lengths of the spacers are beneficial for an effective face-to-face π–π interaction between their PDI units (centroid-to-plane distance of ca. 3.31 Å). Therefore, the **PEPb**-**PBPb** pair **1b** is first arranged in a criss-cross formation, which shows rotational displacements of 42° between the stacked PDI units. Then, two **1b** dimers are stacked on top of each other through π–π interactions between two PDI units from the shorter **PEPb** molecules (centroid-to-plane distance of 3.34 Å, Figure 1a). There is a total of 32 butyl chains that stretch around the tetramer complex **2b** to prevent further stacking. Hence, only weak van der Waals interactions exist between the rectangular tetramer assemblies, which make **2b** closely pack into a layer in the crystallographic (1 0 1) plane (Figure 1d). The layers stack further, following the ABAB sequence of cubic closet packing. Note that highly disordered lattice solvent molecules fill up the space, accounting for stable single crystals.

The formation of stable discrete π-aggregates in MCH was confirmed from dynamic light scattering (DLS) experiments. For the solutions of **PEPa** and **PBPa** individually (0.2 mM), the average hydrodynamic diameter (d_H) values of the corresponding π-aggregates were determined to be 226 nm and 444 nm, respectively (Figure 2). Upon addition of 0.5 and 1 equivalent of **PBPa** to the solution of **PEPa** (0.2 mM), the measured d_H values decreased to 115 and 2 nm, respectively. Notably, the π-aggregates with a mean size of 2 nm have a rather narrow size distribution. Moreover, for the solutions of **PEPa**/**PBPa** at two different concentrations (0.1

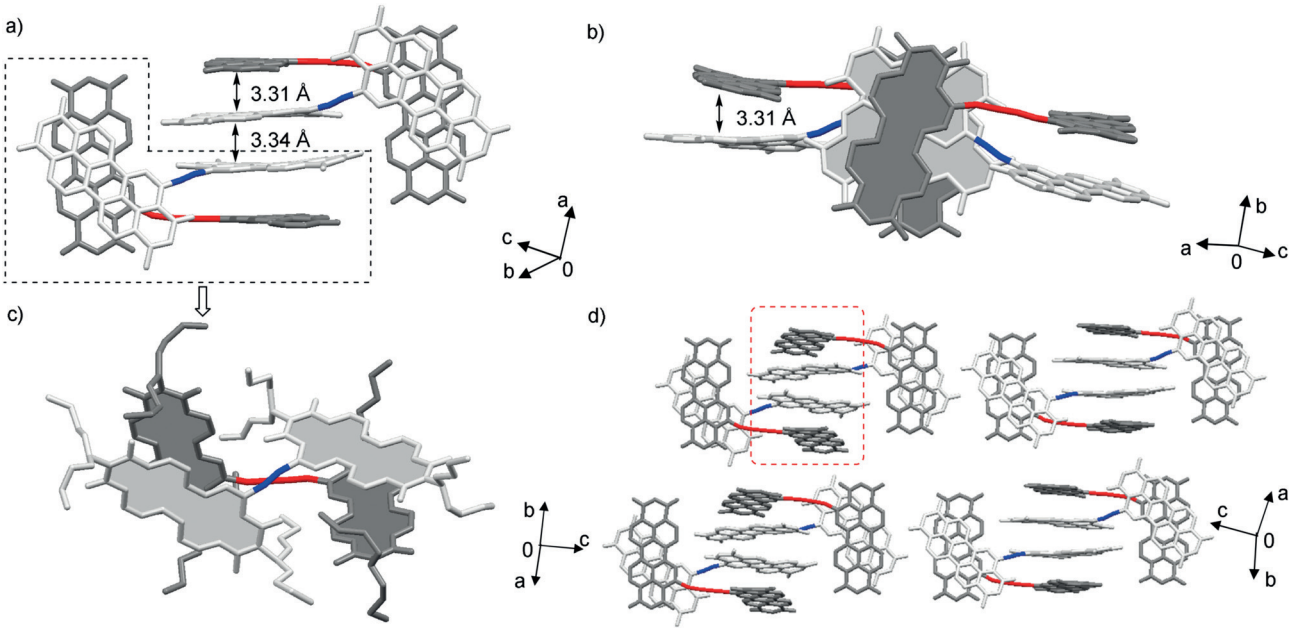

Figure 1. a,b) ORTEP structure of **2b** (front and top views). c) **PEPb**-**PBPb** pair in a criss-cross arrangement. d) Packing modes of **2b** in a stacked layer. The blue- and red-colored bonds represent ethynylene and butadiyne spacers, respectively. For clarity, butylpentyl groups in a), b) and d) and all H atoms are omitted.

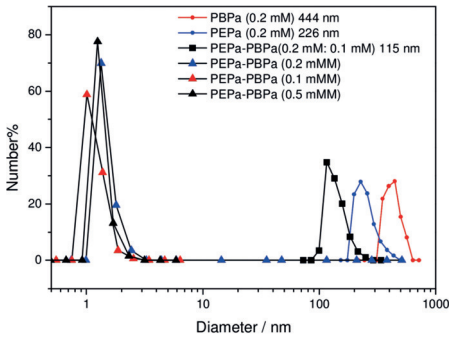

Figure 2. DLS results of **PEPa** (0.2 mM), **PBPa** (0.2 mM), and **PEPa**/**PBPa** mixtures in MCH.

and 0.5 mM, both for each components), the average diameters of the π-aggregates are also close to 2 nm.

To further characterize the size of the aggregates at higher concentrations (> 0.5 mM) that were unsuitable for DLS measurements, diffusion ordered NMR spectroscopy (DOSY) studies were performed on **PEPa**/**PBPa** (1:1) in [D_{14}]MCH. Bulky 1,3,5-tri-*tert*-butylbenzene (TTB) was used as an internal reference to eliminate contributions from solution viscosity, which tend to vary with temperature change as well as aggregation.[10]

The ratio d_m/d_{TTB}, where d_m and d_{TTB} are the average d_H of the main species (i.e., monomeric forms of **PEPa**, **PBPa**, and their aggregates) and TTB, respectively, was used to estimate the size and extent of aggregation of the main species in solution. According to the Stokes-Einstein equation, for rodlike and spherical molecules, the ratio d_m/d_{TTB} is inversely proportional to the ratio of the measured diffusion coefficients (D_m/D_{TTB}).[11] DOSY experiments on equimolar solutions of **PEPa**/**PBPa**, at concentrations of 0.5 mM, 1 mM, 5 mM and 10 mM, resulted in concentration-independent D_m/D_{TTB} values around 4.3 (see Figure S3). Because the bulky TTB only exists as monomer in solution, its hydrodynamic diameter d_{TTB} can be calculated from the crystal structure (about 7.2 Å; see Figure S4). Accordingly, a 4.3-fold larger effective size of the main species implies that the value of d_m is 3 nm. Remarkably, signals that are not resolved in the frequency domain exhibit the same diffusion coefficient, indicating the formation of a single main aggregate species in solution.

Combining the results of DLS and DOSY experiments, we can exclude the possibility of the formation of extended π-stacks and conclude that uniform, discrete π-aggregates are formed. However, DLS and DOSY are unable to distinguish between the dimer **1a** and tetramer **2a**, because of their limited resolution.[12] To further elucidate the structure of the **PEPa**/**PBPa** aggregates obtained in solution, we performed ^{1}H NMR measurements. Crystal structures, obtained on **2b** as shown in Figure 1c,d, suggest that the two PDI units of **PEPa** should be equivalent in the dimer **1a**, whereas they should experience a different environment in the tetramer **2a**. Temperature-dependent NMR spectroscopy on **PEPa**/**PBPa** (10 mM) in [D_{14}]MCH at 353 K revealed two sets of PDI signals in the perylene region, occurring in a 14:14 ratio and appearing with much better resolution compared to individually dissolved PDI dyads (Figure 3). These two sets indicate that the two PDIs of **PEPa**, as well as the two PDIs of **PBPa**, in the assemblies are equivalent (see Figure S5). Upon gradually cooling the sample, the peaks in these spectra

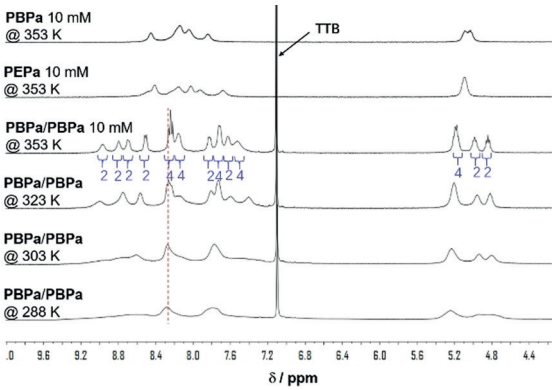

Figure 3. Temperature-dependent ^{1}H NMR analysis of **PEPa**/**PBPa** (10 mM) in [D_{14}]MCH. (TTB: 5 mM as internal reference).

appeared to broaden, probably because the exchange of **1a** with **PEPa** and **PBPa** proceeded at a rate similar to that of the NMR time scale. This trend became more apparent in ^{1}H NMR analyses in less polar [D_8]toluene with relatively faster exchange (see Figure S6). Concentration-dependent ^{1}H NMR results are also consistent with a concentration-independent formation of aggregates. At 0.5 mM, only a simple pattern of proton resonances for **1a** is observed. Along with the increasing of concentration to saturated solution (40 mM), the spectral shape, chemical shifts, and signal number for perylene protons did not change at all (see Figure S7). Together, these results indicate that the dominant species in these solutions is the dimer complex **1a**.

The concentration-independent aggregation behavior of **1** encouraged us to assess the limit of the assemblies' stabilities. To this end, concentration-dependent UV/vis spectra of **1a** were acquired from 200 μM to 1 μM, the detection limit for our molecules in UV/vis spectroscopy. Upon dilution, the spectra did not show any prominent changes, indicating the main species in this concentration range is still the dimer **1a**. The value of $A_{0\text{-}0}/A_{0\text{-}1}$ is maintained at 0.7, which signifies the fully aggregated state of PDI (Figure 4a).[13] To quantify the stability of the assemblies, the monomer-dimer equilibrium model was fitted to the temperature-dependent extinction coefficient values at 514 nm, acquired at different concentrations (Figure 4b; see Figure S8).[14] The fitted thermodynamic constants are as follows: $\Delta H^0 = (-70 \pm 10)$ kJ mol^{-1}, $\Delta S^0 = (-72 \pm 39)$ J K^{-1} mol^{-1}, and $K_{1a} = 3.7 \times 10^8$ M^{-1} at 298 K. The isosbestic points at 486 nm and 527 nm that appear in the temperature-dependent UV/Vis spectra corroborate the two-state equilibrium between free PDI dyads and **1a** dimers. In contrast, **PEPa** as well as **PBPa** form, when not mixed together, H-type aggregates, as evidenced by the reversal of the intensities of the 0-0 and 0–1 absorption bands that was observed in concentration-dependent UV/vis spectra in MCH at 333 K (see Figure S9).[5c] Considering the formation of large sized aggre-

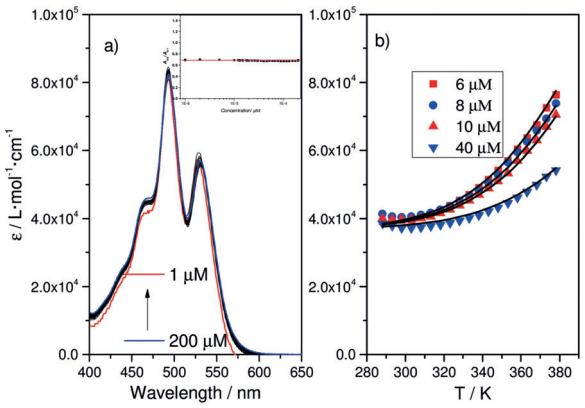

Figure 4. a) Concentration-dependent UV/vis absorption spectra of **1a** in MCH at 298 K (c_0 = 200-1 μM, insert shows the value of $A_{0\text{-}0}/A_{0\text{-}1}$ at different concentrations). b) Plots of UV/vis data points (514 nm) as a function of temperature (6, 8, 10, 40 μM) and fitting with monomer-dimer model.

gates, which is confirmed by the DLS experiments (Figure 2), the isodesmic aggregation model was fitted to the UV/vis data acquired at 524 nm for **PEPa** and **PBPa** (see Figure S10). The binding constants of $K_{PEPa} = 0.93 \times 10^5\,M^{-1}$ and $K_{PBPa} = 1.1 \times 10^5\,M^{-1}$ are much higher in comparison to bindings constants typically reported for normal PDIs with swallow-tailed alkyl side chains, suggesting that the two PDI units in **PEPa** as well as **PBPa** confer an enhanced π-stacking.

The spatially isolated and pairwise arrangements of the PDI dyads in our **1a** dimers provides a potential method to restrict the non-radiative deactivation.[15] Therefore, the fluorescence spectra of **PEPa**, **PBPa**, and **1a** were measured in MCH. For **PEPa** and **PBPa** individually (0.5 μM), the fluorescence spectra showed well-resolved vibronic structures, characteristic for monomeric PDI derivatives (Figure 5a). The quantum yields (QYs) were 64% and 37%, respectively, suggesting that rotation of the PDIs around the central linker induces a decay of the excited state.[16] In contrast, for **1a** (0.25 μM), the spectra displayed a strong red-shifted emission at 600 nm with a longer lifetime of 17.2 ns, as expected for PDI excimers.[17] The QY of this sample is somewhat improved to 65%, as the formation of discrete **1** aggregates potentially restricts the rotation of PDI units and thereby inhibits non-radiative energy transfer.

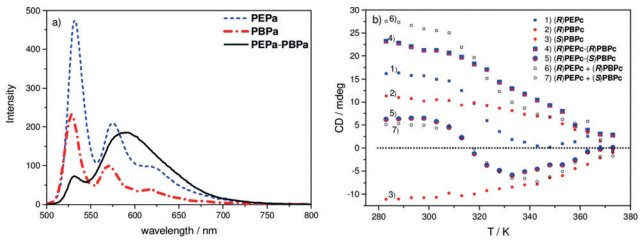

Figure 5. a) Fluorescence (λ_{exc} = 490 nm) spectra of **PEPa** (0.5 μM), **PBPa** (0.5 μM), and **1a** (0.25 μM) in MCH at 298 K. b) Temperature-dependent (283–373 K at 5 K intervals) CD intensities of (***R***)**PEPc**, (***R***)**PBPc**, (***S***)**PBPc**, (***R***)**PEPc**-(***R***)**PBPc**, and (***R***)**PEPc**-(***S***)**PBPc** at 480 nm. Concentration of each components: 2.5 μM in TCE/MCH (1:9).

The strong binding constant of the dimer assemblies (**1**) inspired us to further investigate their chiral recognition properties.[18] (***R***)**PEPc**, (***R***)**PBPc**, and (***S***)**PBPc** with chiral methylheptyl side chains were synthesized for self-assembly studies by circular dichroism (CD) spectroscopy (Figure 5b; see Figure S11). In TCE/MCH (1:9, v:v) solutions, the CD maxima at 480 nm for **(*R*)PEPc** (2.5 μM, Figure 5b-1), **(*R*)PBPc** (2.5 μM, Figure 5b-2), **(*S*)PBPc** (2.5 μM, Figure 5b-3), **(*R*)PEPc-(*R*)PBPc** (2.5 μM: 2.5 μM, Figure 5b-4), and **(*R*)PEPc-(*S*)PBPc** (2.5 μM: 2.5 μM, Figure 5b-5) were plotted versus temperature. The decrease in CD intensity with increasing temperature indicates the transition from the aggregated to the monomeric state. For (***R***)**PEPc**/(***S***)**PBPc** (1:1), the CD of the mixture (Figure 5b-5) matched well with the sum of the spectra of (***R***)**PEPc** and (***S***)**PBPc** (Figure 5b-7), and implies no coaggregation of (***R***)**PEPc** and (***S***)**PBPc** but an orthogonal self-assembly process in the (***R***)**PEPc**/(***S***)**PBPc** mixture. In contrast to (***R***)**PEPc**-(***S***)**PBPc,** the CD value of the (***R***)**PEPc**/(***R***)**PBPc** (1:1) mixture (Figure 5b-4) was different from the sum of the spectra of the components (Figure 5b-6), suggesting strong interactions between (***R***)**PEPc** and (***R***)**PBPc**. This temperature analysis clearly indicates that **PEP** and **PBP**, with the same chirality, prefer the formation of the dimer assemblies, whereas supramolecular conglomerates comprising individual *R* and *S* stacks were formed as a mixture of enantiomers.

In conclusion, we have devised a new host-guest-like aggregation strategy to achieve discrete π-stacks from chromophore look-alikes. With this strategy, two well-designed comparable PDI dyads (**PEB** and **PBP**) that have length-matched linkers can selectively embrace each other through extended π–π interactions to form **PEP-PBP** dimers. In the solid state, the **PEP-PBP** dimers further stack into (**PBP-PEP**)-(**PEP-PBP**) tetramers. In a nonpolar solvent (MCH), the **PEP-PBP** dimers were formed as uniform stacks, even at high concentration (40 mM) or low temperature (278 K). These assemblies feature a high degree of persistence, comparable to the strength of a covalent bond, even at 1 μM. High binding constants of **PEP-PBP** dimers endow them with appealing properties: 1) The high-efficiency and long-lifetime excimer signaling of **PEP-PBP** dimers at long wavelength will enable useful applications as new fluorescent probes and optical materials; 2) The chiral recognition ability of **PEP-PBP** stacks is significant for the development of systems for chirotechnological applications with this important class of functional dyes. Therefore, the presented method provides an excellent approach to engineer well-defined stacks with unique properties and paves the way for reliable studies on structure–property relationships between the chromophores.

Acknowledgements

We are grateful for financial support from the Natural Science Foundation of China (21772162, 21772165, 21572188, 21573118), the Fundamental Research Funds for the Central Universities (20720180031). We gratefully acknowledge Yuanzhi Tan, Hang Qu for X-Ray analysis, Jie Ouyang for

NMR, Xianwen Lou (Tu/e) for MALDI-TOF MS measurements and Qifan Yan for stimulating discussions.

Conflict of interest

The authors declare no conflict of interest.

Keywords: chirality · noncovalent interactions · self-assembly · structure elucidation · supramolecular structures

How to cite: *Angew. Chem. Int. Ed.* **2019**, *58*, 15273 – 15277
Angew. Chem. **2019**, *131*, 15417 – 15421

[1] a) T. Aida, E. W. Meijer, S. I. Stupp, *Science* **2012**, *335*, 813 – 817; b) F. J. M. Hoeben, P. Jonkheijm, E. W. Meijer, A. Schenning, *Chem. Rev.* **2005**, *105*, 1491 – 1546.

[2] a) C. A. Hunter, K. R. Lawson, J. Perkins, C. J. Urch, *J. Chem. Soc. Perkin Trans. 2* **2001**, 651 – 669; b) S. Grimme, *Angew. Chem. Int. Ed.* **2008**, *47*, 3430 – 3434; *Angew. Chem.* **2008**, *120*, 3478 – 3483; c) C. R. Martinez, B. L. Iverson, *Chem. Sci.* **2012**, *3*, 2191 – 2201.

[3] a) T. F. De Greef, M. M. Smulders, M. Wolffs, A. P. Schenning, R. P. Sijbesma, E. W. Meijer, *Chem. Rev.* **2009**, *109*, 5687 – 5754; b) J. K. Klosterman, Y. Yamauchi, M. Fujita, *Chem. Soc. Rev.* **2009**, *38*, 1714 – 1725.

[4] Y. Yamauchi, M. Yoshizawa, M. Akita, M. Fujita, *J. Am. Chem. Soc.* **2010**, *132*, 960 – 966.

[5] a) C. Shao, M. Grüne, M. Stolte, F. Würthner, *Chem. Eur. J.* **2012**, *18*, 13665 – 13677; b) C. Shao, M. Stolte, F. Würthner, *Angew. Chem. Int. Ed.* **2013**, *52*, 7482 – 7486; *Angew. Chem.* **2013**, *125*, 7630 – 7634; c) C. Kaufmann, W. Kim, A. Nowak-Krol, Y. Hong, D. Kim, F. Würthner, *J. Am. Chem. Soc.* **2018**, *140*, 4253 – 4258.

[6] E. Kirchner, D. Bialas, F. Fennel, M. Grune, F. Würthner, *J. Am. Chem. Soc.* **2019**, *141*, 7428 – 7438.

[7] a) F. Würthner, *Chem. Commun.* **2004**, 1564 – 1579; b) W. Jiang, Y. Li, Z. Wang, *Acc. Chem. Res.* **2014**, *47*, 3135 – 3147; c) F. Würthner, C. R. Saha-Möller, B. Fimmel, S. Ogi, P. Leowanawat, D. Schmidt, *Chem. Rev.* **2016**, *116*, 962 – 1052.

[8] a) L. Zhang, D. He, Y. Liu, K. Wang, Z. Guo, J. Lin, H.-J. Zhang, *Org. Lett.* **2016**, *18*, 5908 – 5911; b) J. Wu, D. He, L. Zhang, Y. Liu, X. Mo, J. Lin, H.-J. Zhang, *Org. Lett.* **2017**, *19*, 5438 – 5441; c) J. Wu, D. He, Y. Wang, F. Su, Z. Guo, J. Lin, H.-J. Zhang, *Org. Lett.* **2018**, *20*, 6117 – 6120.

[9] a) Q. Yan, D. H. Zhao, *Org. Lett.* **2009**, *11*, 3426 – 3429; b) Q. Yan, K. Cai, D. H. Zhao, *Phys. Chem. Chem. Phys.* **2016**, *18*, 1905 – 1910.

[10] G. Barozzino Consiglio, P. Queval, A. Harrison-Marchand, A. Mordini, J.-F. Lohier, O. Delacroix, A.-C. Gaumont, H. Gérard, J. Maddaluno, H. Oulyadi, *J. Am. Chem. Soc.* **2011**, *133*, 6472 – 6480.

[11] Y. Cohen, L. Avram, L. Frish, *Angew. Chem. Int. Ed.* **2005**, *44*, 520 – 554; *Angew. Chem.* **2005**, *117*, 524 – 560.

[12] The diameters of **1a** and **2a** are about 2.5 nm and 3.4 nm, respectively, based on the single-crystal X-ray structure analysis of **2b**.

[13] P. Spenst, R. M. Young, B. T. Phelan, M. Keller, J. Dostál, T. Brixner, M. R. Wasielewski, F. Würthner, *J. Am. Chem. Soc.* **2017**, *139*, 2014 – 2021.

[14] Q. Yan, Y. Zhou, Y.-Q. Zheng, J. Pei, D. Zhao, *Chem. Sci.* **2013**, *4*, 4389 – 4394.

[15] H. Liu, L. Yao, B. Li, X. Chen, Y. Gao, S. Zhang, W. Li, P. Lu, B. Yang, Y. Ma, *Chem. Commun.* **2016**, *52*, 7356 – 7359.

[16] M. D. Peeks, P. Neuhaus, H. L. Anderson, *Phys. Chem. Chem. Phys.* **2016**, *18*, 5264 – 5274.

[17] The hypsochromic shift of excimer emission maxima reflects the difference in electronic coupling between the two PDIs in the **PEP-PBP** stacks that leads to excimer state stabilization. See: S. K. M. Nalluri, J. Zhou, T. Cheng, Z. Liu, M. T. Nguyen, T. Chen, H. A. Patel, M. D. Krzyaniak, W. A. Goddard, M. R. Wasielewski, J. F. Stoddart, *J. Am. Chem. Soc.* **2019**, *141*, 1290 – 1303.

[18] M. M. Safont-Sempere, P. Osswald, K. Radacki, F. Würthner, *Chem. Eur. J.* **2010**, *16*, 7380 – 7384.

Manuscript received: June 24, 2019
Revised manuscript received: August 16, 2019
Accepted manuscript online: August 22, 2019
Version of record online: September 12, 2019

